

**NOTICE**

**PORTIONS OF THIS REPORT ARE ILLEGIBLE. It  
has been reproduced from the best available  
copy to permit the broadest possible avail-  
ability.**

**THE ROLE OF CRACK ARREST IN THE EVALUATION OF PWR  
PRESSURE VESSEL INTEGRITY DURING PTS TRANSIENTS\***

R. D. Cheverton      D. G. Ball      CONF-8406165--1

Oak Ridge National Laboratory  
Oak Ridge, Tennessee 37831

CONF-8406165--1

DE84 014076

**ABSTRACT**

The PWR pressurized thermal-shock (PTS) issue, which is concerned with the integrity of the reactor pressure vessel during postulated overcooling transients, is under intensive investigation by the USNRC. The USNRC-sponsored Integrated Pressurized Thermal-Shock (IPTS) and Heavy-Section Steel Technology (HSST) Programs are dedicated to a better understanding and a timely resolution of the problem.

The HSST program is investigating flaw behavior in large cylinders and is also obtaining fracture-mechanics-related material properties, while the IPTS program is primarily concerned with an estimation of the overall frequency of vessel failure and identification of dominant transients and design and operating features contributing thereto for specific nuclear plants. One important component of the IPTS study is a probabilistic fracture-mechanics analysis of the reactor vessel, and a point of particular interest therein is the role of crack arrest in mitigating the consequences of the postulated PTS transients.

The HSST program has provided crack-arrest data from small specimens and large thermally and pressure-loaded cylinders that tend to establish the validity of the crack-arrest concept for application to the PTS problem. Unfortunately, recent results of the IPTS studies indicate that the inclusion of crack arrest in the probabilistic fracture-mechanics model does not substantially influence the calculated frequency of vessel failure. However, there are still significant questions regarding flaw behavior at upper-shelf temperatures, and the HSST program is continuing to pursue this area of uncertainty.

---

\* Research sponsored by the Office of Nuclear Regulatory Research, U.S. Nuclear Regulatory Commission under Interagency Agreements 40-551-75 and 40-552-75 with the U.S. Department of Energy under Contract DE-AC05-84OR21400 with Martin Marietta Energy Systems, Inc.

By acceptance of this article, the publisher or recipient acknowledges the U.S. Government's right to retain a nonexclusive, royalty-free license in and to any copyright covering the article.

## **DISCLAIMER**

This report was prepared as an account of work sponsored by an agency of the United States Government. Neither the United States Government nor any agency thereof, nor any of their employees, makes any warranty, express or implied, or assumes any legal liability or responsibility for the accuracy, completeness, or usefulness of any information, apparatus, product, or process disclosed, or represents that its use would not infringe privately owned rights. Reference herein to any specific commercial product, process, or service by trade name, trademark, manufacturer, or otherwise does not necessarily constitute or imply its endorsement, recommendation, or favoring by the United States Government or any agency thereof. The views and opinions of authors expressed herein do not necessarily state or reflect those of the United States Government or any agency thereof.

## 1. INTRODUCTION

The PWR pressurized thermal-shock (PTS) issue has been under intensive investigation by the USNRC at ORNL since December 1980, at which time ORNL, as a part of the HSST program, initiated a PWR pressure-vessel generic fracture-mechanics analysis pertaining to the Rancho Seco transient that occurred on March 20, 1978.<sup>1</sup> The results of this study<sup>2</sup> indicated that primary-system pressure and temperature transients of the type that were believed to have occurred at Rancho Seco could challenge the integrity of some PWR vessels late in life. Studies of transients at other plants followed, and by May 1981 the NRC had established the Integrated Pressurized Thermal-Shock (IPTS) Program at ORNL. An objective of this program was to estimate the frequency of vessel failure for specific PWR plants, and this effort required the postulation of overcooling transients, an estimate of their frequencies, a thermal-hydraulic analysis of these transients to obtain the primary-system pressure and downcomer coolant temperature as a function of time, and finally a probabilistic fracture-mechanics analysis using these pressure and temperature transients as input.

Fracture-mechanics studies conducted some time ago indicated that under PTS loading conditions very shallow preexistent inner-surface flaws could initiate and propagate in a frangible manner, but in some cases crack arrest could be instrumental in preventing excessive penetration of the vessel wall. However, these studies also indicated that in most cases crack arrest would have to take place in a rising  $K_I$  field ( $dK_I/da > 1$ ) and/or at temperatures above that corresponding to the onset of the Charpy (CVN) upper shelf, which would require  $K_{Ia}$  values higher than had been measured in the lab with small specimens.

Crack arrest behavior under PTS loading conditions has been under investigation at ORNL as a part of the USNRC-sponsored HSST program, and recent experiments associated therewith have involved arrest in a rising  $K_I$  field and arrest on the upper shelf. Furthermore, one of the IPTS-program specific-plant (Oconee-1) probabilistic studies has been completed, and two others (Calvert Cliffs and H. B. Robinson) are well under way. Thus, it is possible, appropriate, and the purpose of this paper to re-examine the role of crack arrest in preventing vessel failure during postulated PTS transients. In doing so, this paper also describes the crack-arrest model that is being used at ORNL for the IPTS studies and reviews relevant crack-arrest data from compact specimens and large test cylinders that indicate the validity of the crack-arrest concept.

## 2. FRACTURE-MECHANICS MODEL

The probabilistic fracture-mechanics calculations for the IPTS program are being performed with the computer code OCA-P,<sup>3</sup> which is based on LEFM and makes use of Monte Carlo methodologies for computing probabilities associated with flaw behavior. Two of the parameters simulated

in the probabilistic analysis are the crack-initiation toughness,  $K_{Ic}$ , and the crack-arrest toughness,  $K_{Ia}$ . Mean values of these parameters are obtained from

$$\bar{K}_{Ic} = 1.43\{36.5 + 3.084 \exp [0.036 (T - RTNDT + 56)]\} \quad (1)$$

$$\bar{K}_{Ia} = 1.25\{29.5 + 1.344 \exp [0.0261 (T - RTNDT + 89)]\}, \quad (2)$$

where

$\bar{K}_{Ic}$ ,  $\bar{K}_{Ia}$  = mean values of initiation and arrest toughness, MPa  $\sqrt{m}$ ;

T = temperature at tip of flaw,  $^{\circ}\text{C}$ ;

RTNDT =  $RTNDT_0 + \Delta RTNDT$  = nil ductility reference temperature,  $^{\circ}\text{C}$ ;

$RTNDT_0$  = initial (zero fluence) value of RTNDT,  $^{\circ}\text{C}$ ;

$\Delta RTNDT$  = increase in RTNDT due to radiation damage,  $^{\circ}\text{C}$ .

Equations (1) and (2) represent the ASME Sect. XI lower-bound curves<sup>5</sup> times a constant. The constants were derived by specifying a normal distribution, one standard deviation ( $\sigma$ ) = 0.15  $\bar{K}_{Ic}$ , 0.10  $\bar{K}_{Ia}$  and by assuming that the ASME lower-bound curves represent  $-2\sigma$  values. These specific values of  $\sigma$  were based on the data that were used to generate the ASME  $K_{Ic}$  and  $K_{IR}$  curves.

A provision is made in OCA-P for limiting  $K_{Ia}$  to some maximum value,  $(K_{Ia})_{\max}$ . One way to select a value of  $(K_{Ia})_{\max}$  is to use a  $K_J$  value corresponding to the upper portion of an appropriate  $J$  vs  $\Delta a$  curve ( $J$ -resistance curve), as illustrated in Fig. 1. This figure shows the radial distribution of fracture toughness through the wall of the vessel at some time during a typical postulated transient. At temperatures less than  $T_D$ , it is assumed that the flaw will behave in a frangible manner only; that is, ductile tearing is not permitted following arrest. [Depending on the value of  $(K_{Ia})_{\max}$  selected, tearing might actually occur and lead to failure.] In accordance with this model, the load line will not intersect the steeply rising portion of the  $J$ - $\Delta a$  curve. Thus, it is sufficient to extend  $(K_{Ia})_{\max}$  across the  $T_D$  line as shown. It is then possible in the analysis for crack arrest to take place on the upper shelf, if the load line rises steeply enough to miss the knee of the  $K_{Ia}$  curve and then drops back down again, as it does for some of the postulated PTS transients.

A particular  $J$ - $\Delta a$  curve of interest corresponds to a specific low-upper-shelf weld [referred to as 61W (Ref. 6)] that was irradiated to a fluence of  $\sim 1.2 \times 10^{19}$  neutrons/cm<sup>2</sup> at a temperature of  $\sim 290^{\circ}\text{C}$  and was tested at  $\sim 200^{\circ}\text{C}$ . The upper portion of the curve is essentially horizontal and equivalent to a  $K_J$  value of  $\sim 220$  MPa  $\sqrt{m}$ . This value has been used for  $(K_{Ia})_{\max}$  in the IPTS studies. As illustrated later, a value of 220 MPa  $\sqrt{m}$  nearly corresponds to the CVN onset of upper-shelf temperature; thus, minimal ductile tearing would be expected at lower values.

$K_{Ia}$  data obtained from wide-plate tests in Japan<sup>7</sup> and pressurized thermal-shock experiments with large cylinders at ORNL<sup>8</sup> indicate that values of  $K_{Ia}$  substantially greater than 220 MPa  $\sqrt{m}$  might be achieved in a PWR vessel. However, the tearing resistance following arrest probably would not be sufficient to prevent ductile tearing up to the point indicated in Fig. 1. Additional experiments are planned as a part of the HSST program to further explore the behavior of flaws under high loading conditions and at temperatures close to and above those corresponding to the onset of upper shelf. Furthermore, calculations have been made to determine the effect of higher values of  $(K_{Ia})_{max}$  on the probability of vessel failure. The results of these calculations are discussed later in the paper.

### 3. VALIDITY OF STATIC CRACK-ARREST CONCEPT FOR PTS STUDIES

The validity of the static crack-arrest concept for application to the PTS issue has been investigated at ORNL by comparing small-specimen crack-arrest data with  $K_{Ia}$  values deduced from a series of thermal-shock and pressurized thermal-shock experiments (TSE-4,<sup>9</sup> TSE-5, -5A and -6,<sup>10</sup> PTSE-1<sup>8</sup>). In most cases the lab  $K_{Ia}$  data were obtained using 25 x 151 x 151-mm wedge-loaded, compact, crack-arrest specimens; and the source of material was a prolongation from each of the test cylinders. (Battelle Columbus Laboratory was responsible for making the small-specimen  $K_{Ia}$  measurements.)

The material used in the testing was a low-alloy forging-grade steel [A508 with class-2 chemistry<sup>11</sup> (see Table 1)] that is used for LWR pressure vessels. Three different heats of material and four different heat treatments were involved. The test cylinders for TSE-5, -5A and -6 came from one heat of material (a single long forging), while the other two test cylinders were from two other heats. The heat treatments differed only in the "tempering" temperature. Preceding tempering, the material was normalized for 8 h at 930°C, air cooled, austenitized for 9 h at 860°C, and then quenched in water. "Tempering" temperatures corresponding to each of the experiments are included in Table 2, which summarizes the test conditions and results. As indicated in the table, test cylinders for four of the five tests (TSE-4, -5, -6, and PTSE-1) were in essentially the quench-only condition. The test cylinder for TSE-5A was tempered at a high enough temperature to nearly satisfy the strength requirements for class-2 material.

Following the water-quench and prior to tempering, sufficient surface material was removed from the test cylinders and their prolongations to avoid having significant residual stresses and gradients in toughness in the sections of material to be tested.<sup>13</sup>

Values of RTNDT for the different test cylinders and their prolongations are also included in Table 2. Because of the different heat treatments and heats of material involved, there is a substantial range in values (10 to 91°C).

A total of 55 small-specimen  $K_{Ia}$  values were obtained as a part of the test-cylinder characterization studies,<sup>14,15</sup> and the thermal-shock experiments produced twelve critical values of  $K_I$  corresponding to crack-arrest events. The small-specimen  $K_{Ia}$  values covered a range of testing temperatures ( $T - RTNDT$ ) of -66 to +59°C, while the corresponding range for the cylinder tests was -30 to 77°C. The twelve  $K_{Ia}$  values deduced from the thermal-shock experiments are plotted in Fig. 2, where they are compared with the ASME Sect. XI  $K_{Ia}$  ( $K_{IR}$ ) curve and the 5 and 95 percentile curves corresponding to a BCL data base of 233  $K_{Ia}$  values for A533 and A508 material. With the exception of a few relatively high data points associated with fracture surfaces having a high density of un-cracked ligaments, the BCL 5 and 95 percentile curves represent lower and upper bounds of the 55  $K_{Ia}$  values obtained from the thermal-shock test-cylinder characterization studies (these 55 values are included in the BCL data base).

Also included in Fig. 2 are three  $K_{Ia}$  values deduced from a French thermal-shock experiment<sup>16</sup> and five values obtained by the Japanese from wide-plate tests,<sup>7</sup> which, like the ORNL pressurized thermal-shock experiment (PTSE-1),<sup>8</sup> permits the investigation of crack arrest at relatively high temperatures.

As indicated by Fig. 2, the scatter in the small-specimen data, with the exception of the few outliers mentioned above, is  $\approx 45\%$  over the temperature range shown, and only a small fraction of the data points falls below the  $K_{IR}$  curve. All of the  $K_{Ia}$  values deduced from the ORNL thermal-shock experiments fall within the small-specimen scatter band and well above the  $K_{IR}$  curve, while the three French data points cluster about the  $K_{IR}$  curve.

The first crack-arrest events during TSE-5A and TSE-6 and both crack-arrest events during PTSE-1 took place in a rising  $K_I$  field ( $dK_I/da > 0$ ), and it is not evident that this resulted in  $K_{Ia}$  values different from those obtained with  $dK_I/da < 0$ , which is the usual condition when obtaining small-specimen  $K_{Ia}$  values. Because of this and the good agreement between the small-specimen and large-cylinder data, it appears that the LEFM crack-arrest concept based on small-specimen data is reasonably valid and can be used with confidence in evaluating the integrity of PWR pressure vessels during postulated PTS transients. Furthermore, the data in Fig. 2 indicate that it would be appropriate to use a higher mean curve in the IPTS probabilistic fracture-mechanics analyses than that expressed by Eq. (2). In the next section of this paper the effect of using a higher value is discussed.

With reference to Figs. 2 and 6, it is also of interest to note that the CVN onset of upper-shelf temperature corresponds to a mean value of  $K_{Ia}$ , based on the large-specimen data, of nearly 200 MPa  $\sqrt{m}$ . This indicates that little, if any, ductile tearing would take place at  $K_I$  values less than the  $(K_{Ia})_{max}$  value selected for the IPTS studies.

#### 4. BEHAVIOR OF INNER-SURFACE FLAWS DURING PTS TRANSIENTS

A fracture-mechanics analysis of the Oconee-1<sup>17</sup> vessel, based on the model described earlier, indicates that for some postulated high-pressure transients axially oriented inner-surface flaws with a maximum surface length of  $\sim 2$  m (height of a shell course) will propagate through the vessel wall without arresting, as indicated by the set of critical-crack-depth curves in Fig. 3.\* Furthermore, increasing the value of  $(K_{Ia})_{max}$  above 220 MPa  $\sqrt{m}$  does not affect this result, provided that Eq. (2) is appropriate for extrapolating to higher values of  $K_{Ia}$ . For an increase in  $(K_{Ia})_{max}$  to have an ameliorating effect, the  $K_{Ia}$  vs  $T$  curve would have to turn up more abruptly.

For a somewhat more severe transient than that associated with Fig. 3 it is possible, as shown in Fig. 4, for crack arrest to take place, if  $(K_{Ia})_{max}$  is increased above 220 MPa  $\sqrt{m}$ . However, the arrest event would take place at or above a temperature corresponding to the onset of the Charpy upper shelf, and thus ductile tearing would be expected as indicated in Fig. 5. If ductile tearing did not take place and if the particular transient extended for  $\sim 30$  min or more beyond the minimum critical time ( $\sim 35$  min), the propagated flaw would reinitiate, and presumably arrest would not take place, as indicated in Fig. 4. Furthermore, if the transient extended as little as  $\sim 10$  min or more beyond the minimum critical time, much shallower flaws could propagate without arresting. Thus, for this transient also, increasing  $(K_{Ia})_{max}$  does not prevent failure, at least for the set of conditions assumed for the particular analysis regarding fluence, fracture-toughness and copper and nickel concentrations.

In the probabilistic fracture-mechanics analysis, parameters that have significant uncertainties associated with them are simulated, and this results in a rather broad range of predicted flaw behavior for a given transient. It is not feasible to examine each of the thousands of cases involved in the manner described above, but it is possible, of course, and instructive to perform the probabilistic fracture-mechanics analysis using different values of  $(K_{Ia})_{max}$  in conformance with the arrest model described in Fig. 1. This has been done for several typical Oconee and Calvert Cliffs postulated transients for a range of  $(K_{Ia})_{max}$  values of 220 to 330 MPa  $\sqrt{m}$ . The results indicate a factor of three decrease in  $P(F|E)$  for some transients and less for many others. Thus, it appears that increasing  $(K_{Ia})_{max}$  will not substantially reduce the calculated frequency of vessel failure.

---

\*The initiation and arrest curves ( $K_I = K_{Ic}$ ,  $K_I = K_{Ia}$ ) in Figs. 3 and 4 are based on the ASME Sect. XI  $K_{Ic}$  and  $K_{Ia}$  curves, and no maximum values were imposed. The inclusion of the 220 MPa  $\sqrt{m}$  iso- $K_I$  curve allows interpretation of the results as if this maximum value were imposed.

Since the data in Fig. 2, which are reproduced in Fig. 6 for illustrative purposes, indicate, when compared to Eq. (2), that a higher mean curve for  $K_{Ia} = f(T - RTNDT)$  could be used in the IPTS studies, the effect on  $P(F|E)$  of doing so was investigated. As indicated in Fig. 6, a better fit to the data is achieved with

$$\bar{K}_{Ia} = 1.75 K_{IR} . \quad (3)$$

Using Eq. (3) for the probabilistic fracture-mechanics analysis of several of the IPTS transients, with  $2\sigma = \pm 0.45 \bar{K}_{Ia}$  and  $(K_{Ia})_{max} = 220 \text{ MPa} \sqrt{m}$ , reduces  $P(F|E)$  for some transients by only a factor of four, and for other transients the reduction is less. Thus, increasing  $\bar{K}_{Ia}$  in the IPTS studies to what appears to be a more realistic value does not substantially reduce the frequency of vessel failure.

Although crack arrest does not appear to play an important role in the evaluation of vessel integrity during postulated PTS transients, there is still considerable uncertainty regarding the behavior of flaws at temperatures close to and corresponding to the upper shelf. Thus, the HSST program will continue to investigate flaw behavior in this temperature regime.

## 5. SUMMARY

Crack-arrest data ( $K_{Ia}$ ) deduced from thermal-shock experiments and wide-plate tests agree very well with lab small-specimen data and generally lie above the ASME Sect. XI  $K_{IR}$  curve. The comparison extends over the temperature range ( $T - RTNDT$ ) of  $-32$  to  $+93^\circ\text{C}$ , and the scatter in the data up to  $\sim 60^\circ\text{C}$  is such that  $2\sigma \approx \pm 45\%$ .

The mean of the above data is about 1.75 times the ASME Sect. XI  $K_{IR}$  curve. This mean curve is substantially higher than the mean curve selected for the IPTS studies on the basis of the small-specimen data that were used to establish the  $K_{IR}$  curve ( $K_{Ia} = 1.75 K_{IR}$  compared to  $1.25 K_{IR}$ ), and the scatter is greater, also ( $2\sigma \approx 0.45 \bar{K}_{Ia}$  compared to  $0.20 \bar{K}_{Ia}$ ).

Unfortunately, inclusion of the higher mean curve in the IPTS studies does not reduce the conditional probability of vessel failure,  $P(F|E)$ , by a significant amount.

The ORNL PTSE-1  $K_{Ia}$  data and the Japanese wide-plate  $K_{Ia}$  data indicate that  $K_{Ia}$  values greater than the maximum value ( $220 \text{ MPa} \sqrt{m}$ ) used in the IPTS studies might actually be achieved. However, recent calculations indicate that  $P(F|E)$  is insensitive to increases in  $(K_{Ia})_{max}$ .

There are still significant uncertainties regarding crack arrest on the upper shelf that could influence the calculated effect of crack arrest on  $P(F|E)$ . Thus, the HSST program is continuing to investigate flaw behavior at elevated temperatures.

## References

1. S. Fabic, Reactor Coolant Pressure and Temperature Data for the March 20, 1978 Cooldown Event at the Rancho Seco Power Plant, memo to C. Z. Serpan, USNRC, November 25, 1980.
2. R. D. Cheverton, "Parametric Analyses of Rancho Seco Overcooling Accident," letter to M. Vagins, USNRC, March 3, 1981.
3. R. D. Cheverton and D. G. Ball, A Deterministic and Probabilistic Fracture-Mechanics Code for Application to Pressure Vessels, NUREG/CR-3618 (ORNL-5991), Union Carbide Corp. Nuclear Div., Oak Ridge Natl. Lab (May 1984).
4. ASME Boiler and Pressure Vessel Code, Section III, Division I, Subsection NA, Appendix I, American Society of Mechanical Engineers, New York, NY, 1974.
5. T. U. Marston (Ed.), Flaw Evaluation Procedures, ASME Section XI, Background and Application of ASME Section XI, Appendix A, Special Report, EPRI NP-719-SR, American Society of Mechanical Engineers, Electric Power Research Institute (August 1978).
6. A. L. Hiser, F. J. Loss, B. H. Menke, J-R Curve Characterization of Irradiated Low Upper-Shelf Welds, NUREG/CR-3506 (MEA-2028), (in preparation).
7. Japan Welding Council, Structural Integrity of Very Thick Steel Plate for Nuclear Reactor Pressure Vessels, JWES-AE-7806, 1977 (in Japanese).
8. R. H. Bryan et al., "Quick-Look Report on the First Pressurized-Thermal-Shock Test, PTSE-1," ORNL/PTSE-1, March 7, 1984.
9. R. D. Cheverton and S. E. Bolt, Pressure Vessel Fracture Studies Pertaining to a PWR LOCA-ECC Thermal Shock: Experiments TSE-3 and TSE-4 and Update of TSE-1 and TSE-2 Analysis, ORNL/NUREG-22, Oak Ridge National Laboratory, Oak Ridge, Tennessee (December 1977).
10. R. D. Cheverton et al., "Fracture Mechanics Data Deduced from Thermal-Shock and Related Experiments with LWR Pressure Vessel Material," Journal of Pressure Vessel Technology, Transactions of the ASME, 102/Vol. 105, May 1983.
11. "Standard Specification for Quenched and Tempered Vacuum-Treated Carbon and Alloy Steel forgings for Pressure Vessels," ASTM, Philadelphia, 1984 (1984 Annual Book of ASTM Standards, Sect. 1, Vol. 01.04).
12. ASME Code, Section XI, Division 1, Subsection NB-2331.
13. D. A. Canonico, "Transition-Temperature Considerations for Thick-Walled Steel Nuclear Pressure Vessels," Nuclear Engineering and Design, Vol. 17, 1971, pp. 149-160.

14. A. R. Rosenfield, "Validation of Compact-Specimen Crack-Arrest Data," Technical Briefs, Journal of Engineering Materials and Technology, Vol. 106/207, April 1984.
15. A. R. Rosenfield et al., Heavy-Section Steel Technology Program Semi-annual Progress Report October-March FY 1984 (in preparation).
16. A. Pellissier-Tanon, P. Sollogoub, B. Houssin, "Crack Initiation and Arrest in an SA 508 Class-3 Cylinder Under Liquid Nitrogen Thermal-Shock Experiment," Transactions of the 7th International Conference on Structural Mechanics in Reactor Technology, Vols. G and H, August 1983.
17. T. J. Burns et al., Pressurized Thermal Shock Evaluation of the Oconee-1 Nuclear Power Plant, NUREG/CR-3770 (ORNL/TM-9176), (in preparation).

Table 1. Chemical composition for A 508 Class 2 material<sup>[11]</sup>

Composition, <sup>a</sup> weight percent									
C	Mn	P	S	Si	Cr	Ni	Mo	V	
0.27	0.50	0.012	0.015	0.15	0.25	0.50	0.55	0.05	
		1.00			0.40	0.45	1.00	0.70	

<sup>a</sup>Single values are maximum.

Table 2. Test conditions and summary of results for ORNL thermal-shock and pressurized thermal-shock experiments

	TSE-4	TSE-5	TSE-5A	TSE-6	PTSE-1
<b>Cylinder dimensions, mm</b>					
Outer diameter	533	991	991	991	991
Inner diameter	242	686	686	838	686
Length	914	1219	1219	1219	1372
<b>Cylinder material</b>					
Type	SA 508 with class-2 chemistry				
Tempering temperature, °C	No tempering <sup>a</sup>	613 <sup>b</sup>	679 <sup>b</sup>	613 <sup>b</sup>	561 <sup>c</sup>
RTNDT, °C	~90 <sup>d</sup>	66 <sup>e</sup>	10 <sup>f</sup>	66 <sup>e</sup>	91 <sup>e</sup>
<b>Flaw (initial)</b>					
Type	Long, inner surface				
Orientation	Longitudinal				
Length, mm	914	1219	1219	1219	1000
Depth, mm	11	16	11	8	11
<b>Thermal Shock</b>					
Cylinder initial temperature, °C	291	96	96	96	290
Coolant initial temperature, °C	-25	-196	-196	-196	-25
Coolant	Alcohol and water	LN <sub>2</sub>	LN <sub>2</sub>	LN <sub>2</sub>	Alcohol and water
Pressure, MPa	0	0	0	0	0.90
<b>Initiation-Arrest Events</b>					
Number	1	3	4	2	2
Arrest depth, mm	22	30, 96, 122	21, 30, 48, 82	21, 142	22, 37
Arrest temperature, °C					
T	126	36, 82, 89	22, 38, 51, 67	34, 64	157, 169
T - RTNDT	36	30, 16, 23	12, 28, 41, 57	32, 2	66, 78
K <sub>1a</sub> , MPa $\sqrt{\text{m}}$	127	86, 104, 92	76 <sup>g</sup> 86, 107, 130	63 <sup>g</sup> 105	177 <sup>g</sup> 265 <sup>g</sup>

<sup>a</sup>Cylinder tested in quenched condition.<sup>e</sup>Based on CVN data. [12]<sup>b</sup>Temperature maintained for 4 h, air cooled.<sup>f</sup>Based on drop weight. [12]<sup>c</sup>Stress-relief treatment only.<sup>g</sup>Rising K<sub>1</sub> field.<sup>d</sup>Corresponds to CVN energy of 40 J. No drop-weight testing; CVN upper shelf less than 68 J.

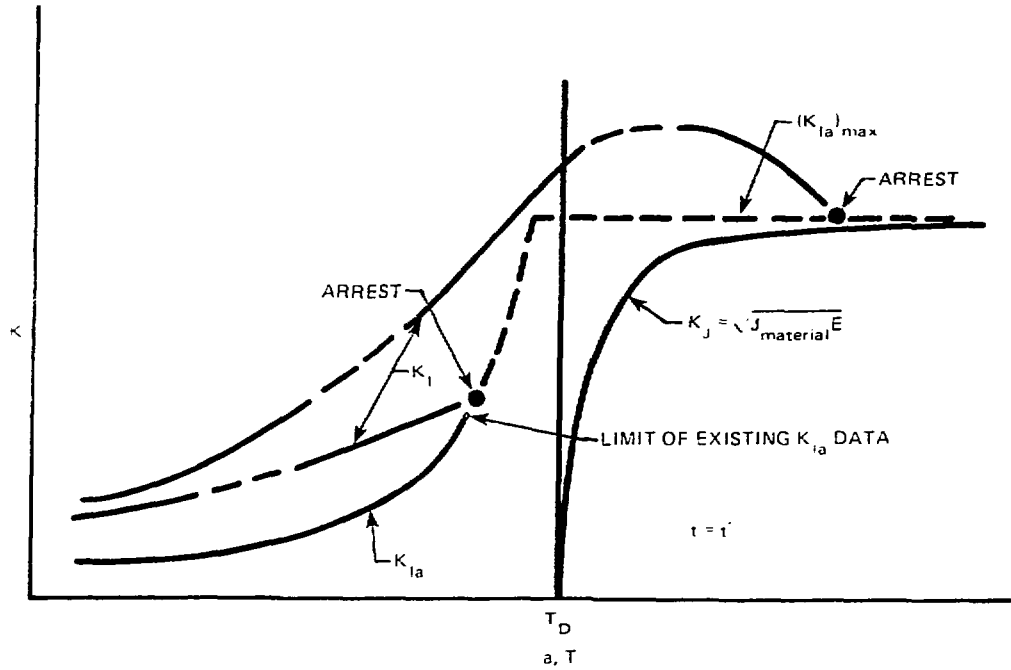
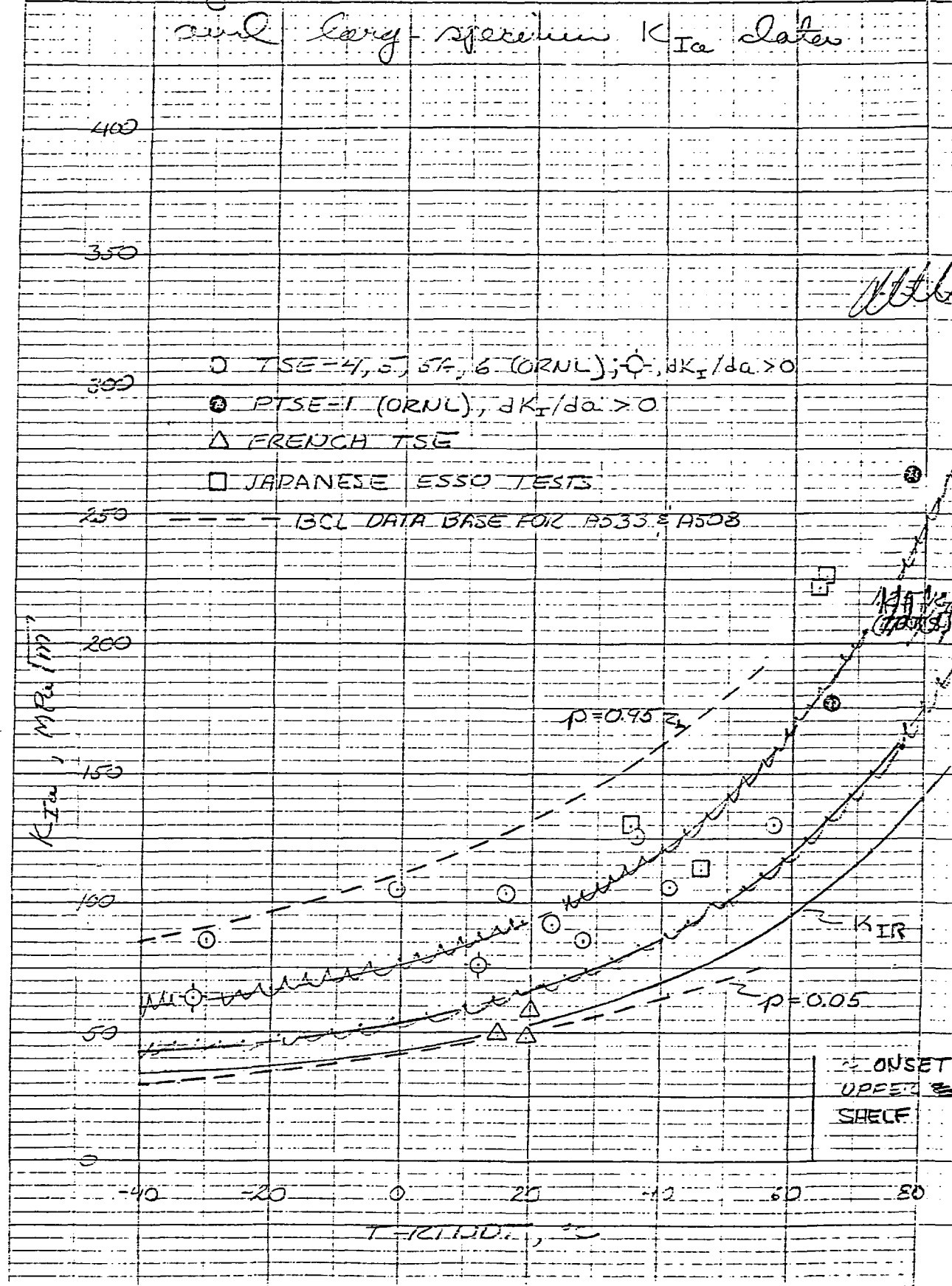


Fig. 1. Illustration of method for selecting  $(K_{Ia})_{max}$ .

Fig 2 Comparison of small-specimen  
and large-specimen  $K_{Ic}$  data 2-4-84

Square 10 x 10 to the inch AS 6000 ft

Graphical method of calculating 'C' constant, 'A' constant  
for use in Eq. 10



CRITICAL CRACK DEPTH CURVES FOR  
RTNDT0 --6.7 DEGC  $\Delta Cu = 0.29$   $\Delta Ni = 0.55$   $F_0 = 1.09E19$  IPTS OCONEE CLAD 6A 10/20/83  
LONGIT

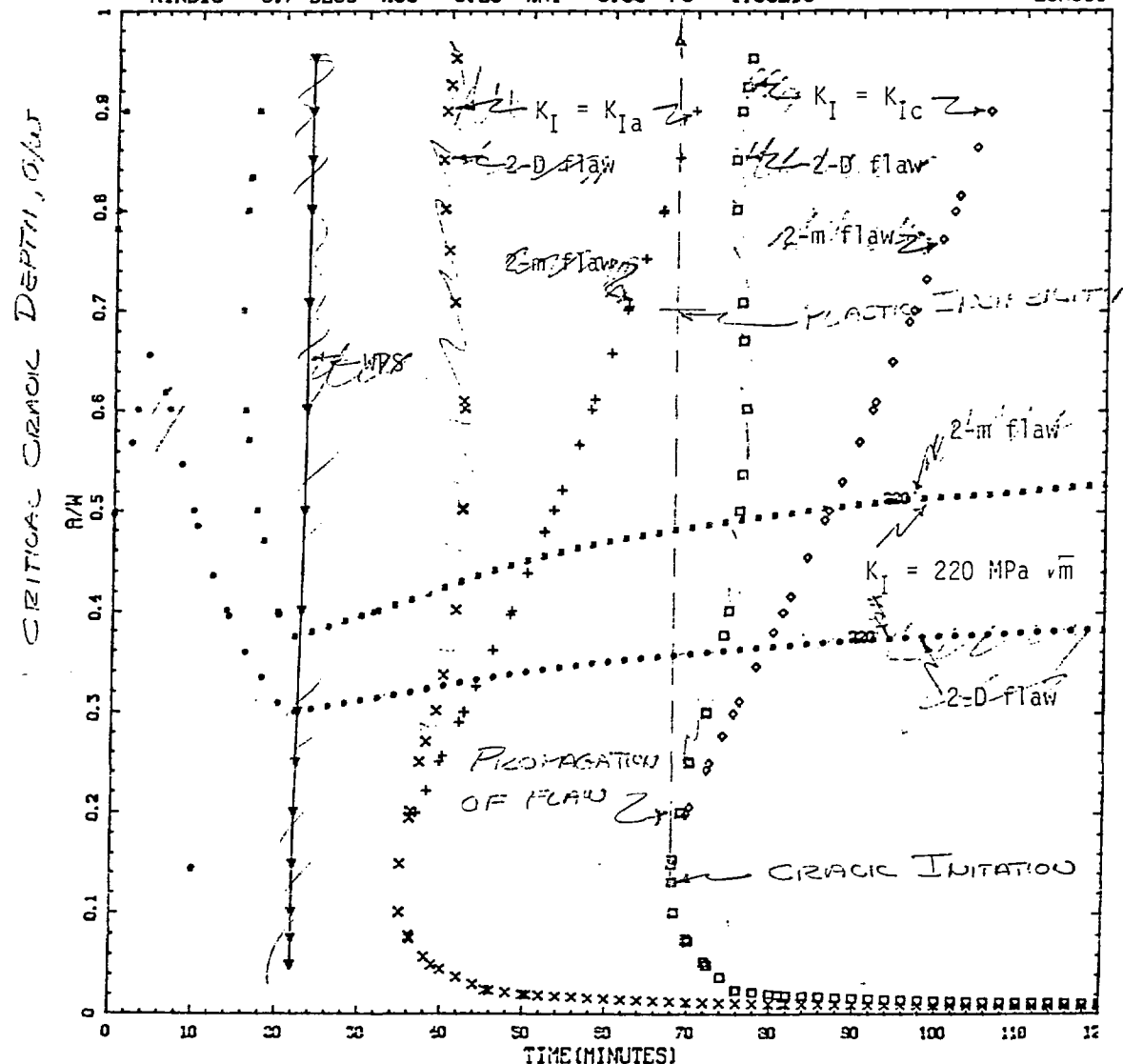


Fig. 117. Critical-crack-depth curves for Oconee-I postulated transient No. 44, 32 EFPY, weld SA1430.

CRITICAL CRACK DEPTH CURVES FOR  
RINOTO -6.7 DEG C ZCU - 0.29 ZNI - 0.55 FO - 1.0E19

IPTS JOONEE CLAD W2TBV 11/04/83

LONGIT

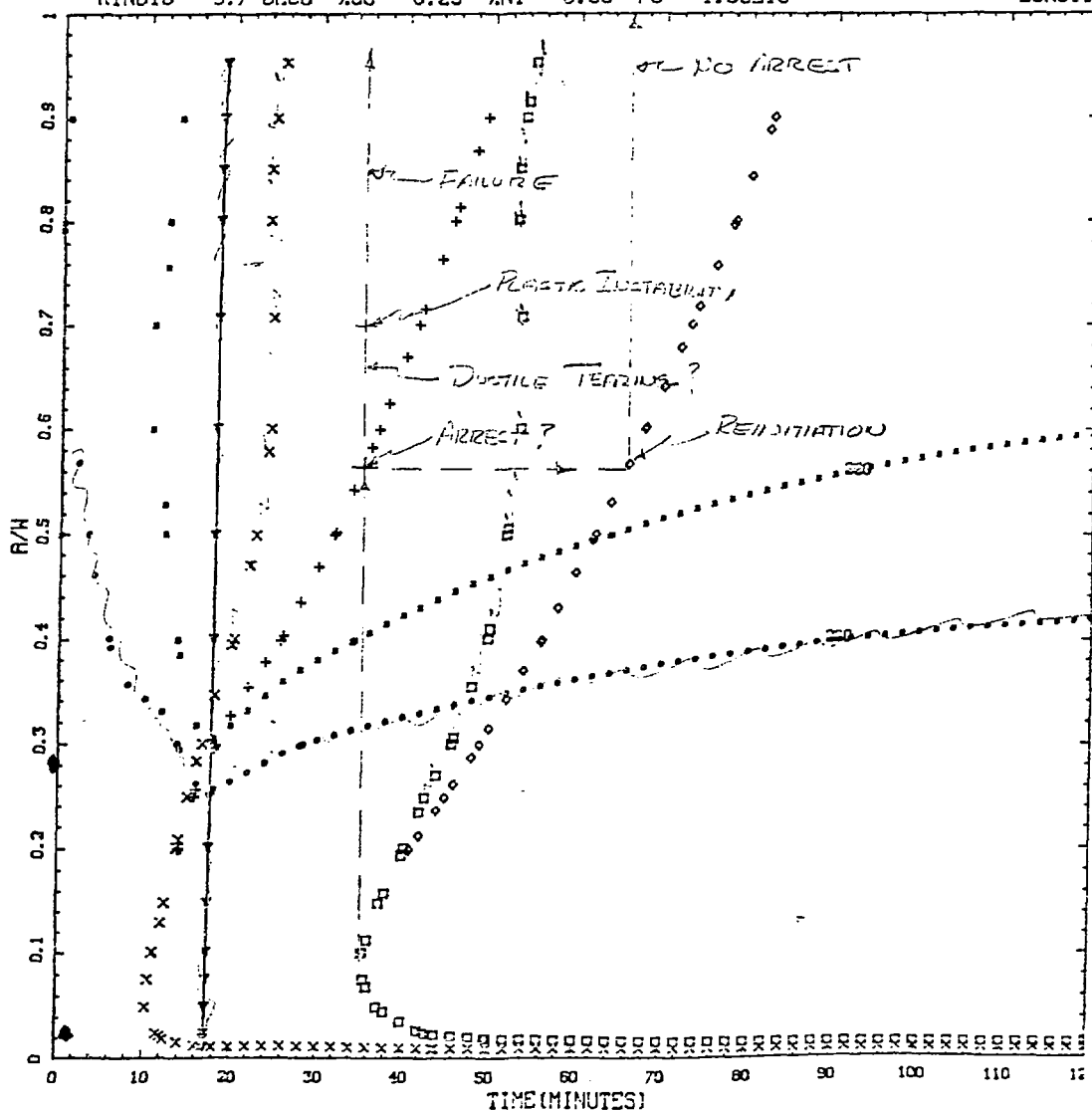


Fig. 4 Critical crack depth curves for Rinoto  
at -6.7°C. Data: 1/2" D234, 32EFPY, 0.25" CLAD

5/8/84

OCEAN-1 112-TBV  $t = 36$  min

Fig. 5 Radial distribution of  
 $K_I$  and  $K_{Ia}$  in tensile crack  
 at a specific time in a  
 PTS specimen

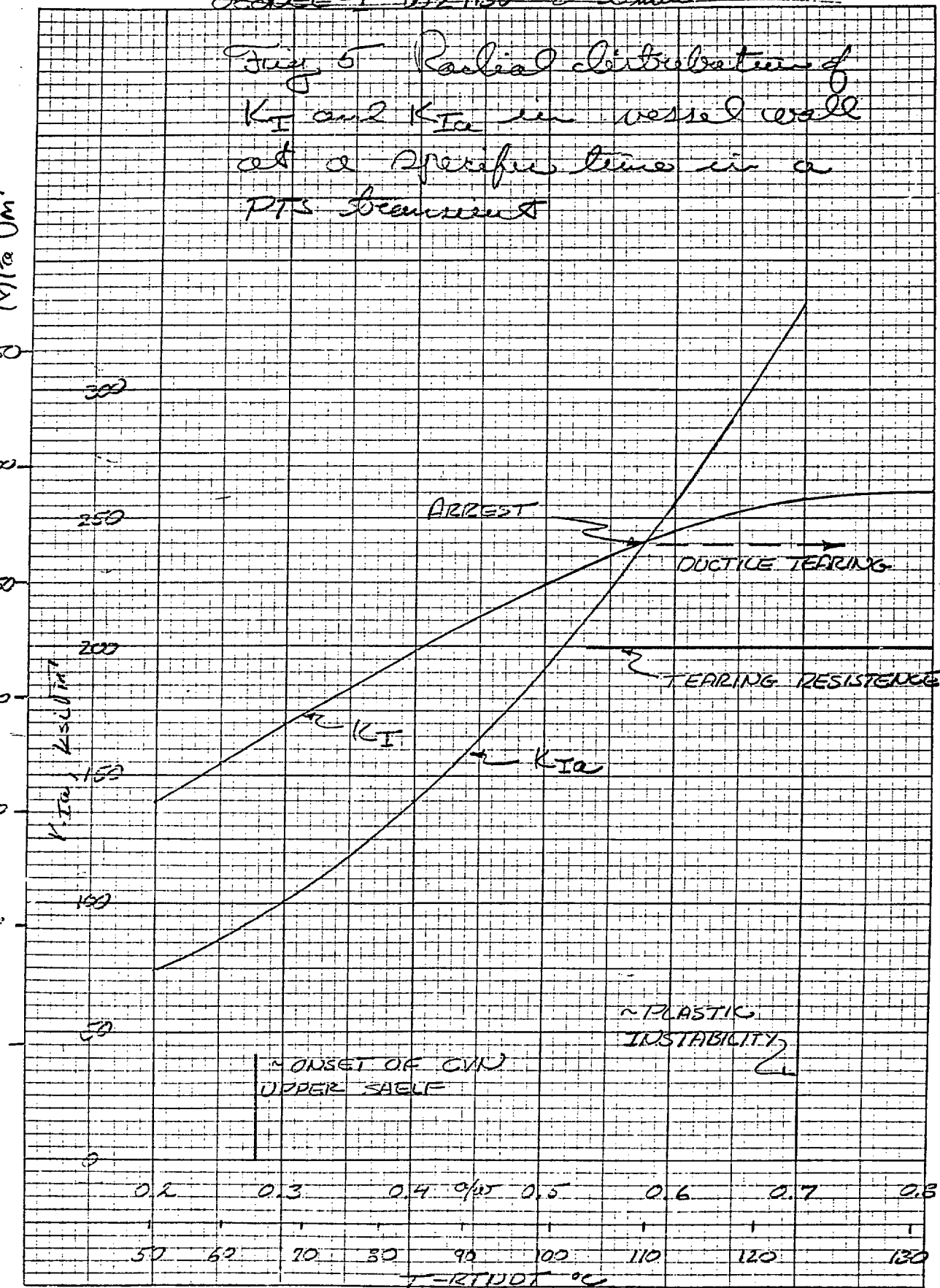
10 x 10 (1) INCH

AS-0007-01

Buffalo, New York

GRAPH PAPER GRAPHIC CONTROLS CORPORATION

Printed in U.S.A.



Aug 6 Comparison of large-specimen 2-4-87

K<sub>1a</sub> data and  $K_{1a} = f(T - RTNDT)$   
covered in IPTS tables

